ENERGY-ABSORBING CHARACTERISTICS ANALYSIS OF COMPOSITE THIN-WALLED C-CHANNELS UNDER LOW SPEED AXIAL COMPRESSION

Jiang XIE*, Zhenyu Feng*, Shanshan SONG*, Dongfang SONG*, Xuehan, ZANG*
*** Key Laboratory of Civil Aircraft Airworthiness Technology, CAAC , Civil Aviation University of China, Tian Jin, P.R. China**

Abstract

Low speed axial compression was conducted on T700/MTM28 composite thin-walled C-channels. The effect of different lay-ups on energy-absorbing properties was investigated by observing the load-displacement curves together with the failure modes. The energy-absorbing properties indicators, such as initial peak load (F_{max}), average crushing load (F_{mean}) and specific energy absorption (SEA), were measured and compared. The results show that the C-channels with unidirectional 0° plies are not beneficial to absorb crushing energy due to the occurrence of global buckling. The C-channels with 0°/90°, ±45° and 45°/90°/-45°/0° lay-ups are found to absorb energy through progressive failure of the structure such as local buckling, delamination, bending and fiber fracture. Moreover, the SEA of C-channels with 45°/90°/-45°/0° lay-up increases as the thickness increases and they hence have a greater potential on energy-absorbing structure design and application.

1 Introduction

Composite materials have been extensively and intensively applied in the primary structure of aircraft due to its low density, high specific strength and designable mechanical properties. Because the impact properties, failure modes and mechanical behaviors of composite material after impact are significantly different from metal, understanding its energy absorbing/dissipating mechanism and using its properties are the preconditions for the design and verification of the composite structure. In recent years, aircraft manufactory (such as Boeing, Airbus and COMAC), airworthiness certification departments (such as FAA and EASA), research institutes and universities (such as DLR, Washington University, etc.) have focused on energy absorption of composite structures by considering trigger [1-4], geometric features [5-7], mechanical properties of fiber and matrix [8] as well as ply lay-up [9,10]. But there are few studies reported on the energy absorbing mechanism of composite C-channels.

In this paper, low-speed axial crushing tests were conducted on the composite thin-wall C-channels with different lay-ups. Failure mode and energy absorbing mechanism of the C-channels were investigated and the effect of ply orientation on crushing energy absorption was discussed.

2 Compression test of composite thin-walled C-channels

2.1 Composite thin-walled C-channels specimens

The C-channels were made of T700/MTM28 carbon fiber reinforced epoxy resin composite. The geometric dimensions of specimen are shown in Fig.1. A 45° chamfer on top end was implemented to reduce the initial peak load. Composite thin-walled C-channels were stacked up to 12 and 16 plies corresponding to 1.8 mm and 2.4 mm in thickness respectively. The detail configurations of specimens are shown in Table 1.

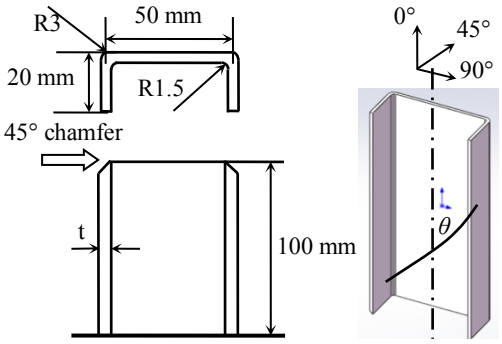

Fig.1 Geometry dimension of composite T700/MTM28 C-channels specimens

Table 1 C-channel configuration parameters

Specimen	Thickness/mm	Ply orientation
C120	1.8	$[0]_{12}$
C121		$[0/90]_{3s}$
C122		$[+45/-45]_{3s}$
C123		$[+45/90/-45/0]_3$
C160	2.4	$[0]_{16}$
C161		$[0/90]_{4s}$
C162		$[+45/-45]_{4s}$
C163		$[+45/90/-45/0]_{2s}$

2.2 Axial compression test of composite thin-walled C-channels

The uniform low-speed axial crushing tests at room temperature were conducted by using the Instron material testing machine (INSTRON VHS 160/100-20). The loading speed was 0.05 m/s, the installation of the test equipment and specimen is illustrated in Fig.2. Furthermore, high-speed video was used to record the crushing process during the entire test.

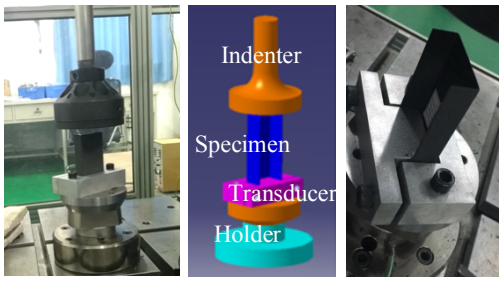

Fig 2 Diagram of the test device

2.3 Result of axial compression test

In the crushing process of C-channels with unidirectional 0° plies, the behavior of specimens C120 and C160 are similar. The specimens are easy to split, as shown in Fig.3, which is because of the absence of circumferential reinforcement. It is found that axial splitting occurs firstly in the corner region, and then initiates fiber bundles into global buckling. The specimens were damaged in an overall unstable failure mode. Specifically, the load-displacement curves of the 0° ply specimen are shown in Fig.4. The crushing load decreases rapidly and remains at a low level after the peak load, resulting in overall instability and the loss of the load-bearing capacity.

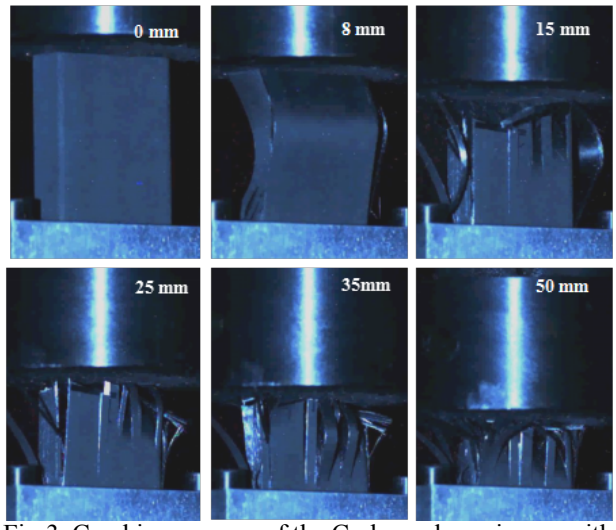

Fig 3. Crushing process of the C-channel specimens with 0° ply

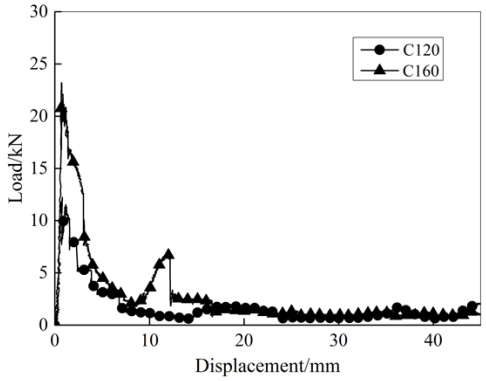

Fig 4. Load-displacement curves of C-channels with 0° plies

Different from C-channels with unidirectional 0° plies, the C-channels stacked by 0°/90° lay-up, C121 and C161, undergo progressive crushing process and gradual failure mode during the low-speed axial crushing test. Under the effect of circumferential reinforcement of 90° fiber, neither global buckling nor overall splitting are observed. Furthermore, a certain rebound after unloading occurs due to the elastic

deformation of 0° plies. The failure morphology of C121 and C161 are shown in Fig.5, it can be seen that fold and collapse occur repeatedly and there is a number of horizontal cracks in the web and flange, along with some 0° fiber detaching. The top of the C-channel and both flanges are delaminated. Fiber and matrix breakage is observed at the corner zone due to stress concentration. When 0° fibers are compressed axially, 90° fibers are unable to provide axial support to the structure and will be pulled off by bended and buckled 0° fibers. On the contrary, in the case of C161, the folding phenomenon is less obvious, meanwhile matrix brittle fracture is dominant. Compared with C121, the thicker C161 is less prone to local buckling, folding and collapse. Additionally, transverse rupture is found at both sides of the flange in the bottom of C161.

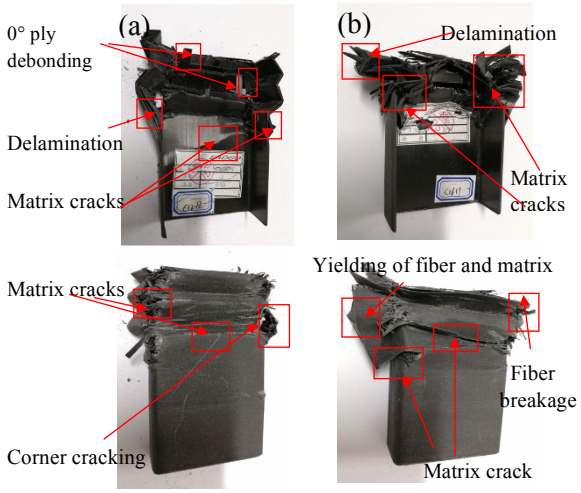

Fig 5. Failure modes of C-channels specimen with 0°/90° ply: (a) C121; (b) C161

The load-displacement curves of the 0°/90° ply C-channel specimen are shown in Fig.6. The initial peak load is larger, showing continuous 'serrated' fluctuations, and the fluctuating amplitude is larger. Moreover, the interval between the peaks of the wave is larger. The load-displacement curve also shows that the average crush load decreases with increasing displacement. In addition, the load-displacement curve of the C161 specimen fluctuates twice from approximately 30 mm, representing two large-scale local buckling failures.

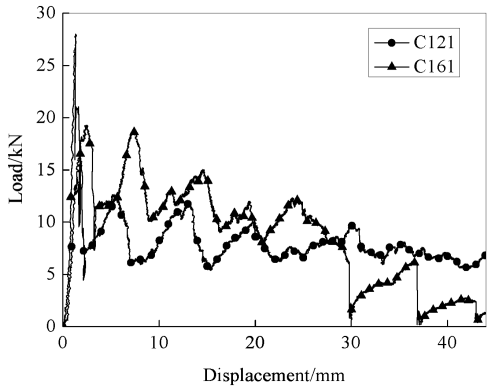

Fig 6. Load-displacement curves of C-channels with 0°/90° plies

In the case of the C-channels with +45°/-45° lay-up, C122 and C162, due to the reinforcement of ±45° fiber, no crack occurs in the corner region meanwhile elastic deformation of fiber is observed, as shown in Fig.7. Local buckling on the web results in the slipping of matrix along the fiber direction and lots of 45° cracks occur. Besides, there is 45° direction matrix crack at one side of the flange in the folding zone and the specimen bends inside.

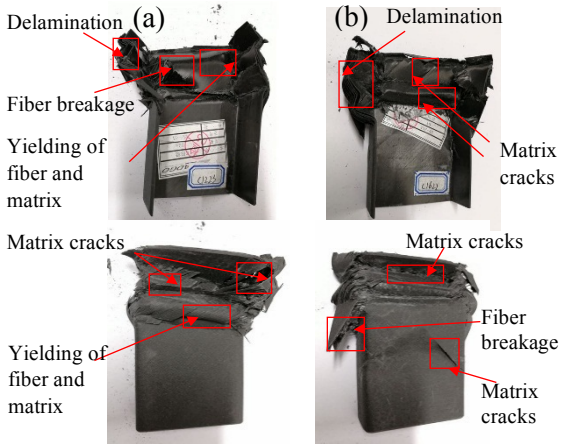

Fig 7. Failure morphology of C-channel specimens with ±45° ply: (a) C122; (b) C162

The load-displacement curves of the ±45° ply C-channel specimen are shown in Fig.8. The initial peak load is small, and the curve shows a nearly 'square wave' shape after the initial peak load. The average crushing load during the crush process does not change obviously.

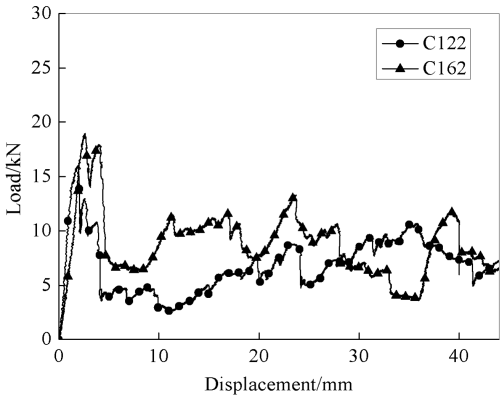

Fig 8. Load-displacement curves of C-channels with 45°/-45° plies

In the case of the C-channels with 45°/90°/-45°/0° lay-up, C122 and C162, the C-channels are able to withstand axial, circumferential and shearing load, so they are collapsed in a stable progressive manner as shown in Fig.9. It can be seen that the crush front is more severely fragmented and failed. It is observed that the failure consists of matrix and fiber fracture as well as debonding of 0° ply in addition to obvious delamination. The crush front is completely fragmented with local buckling, while the lower part of C-channels remains integrity. It is found that the progressive failure beneficial to the energy absorption is achieved by the specimens with 45°/90°/-45°/0° lay-up.

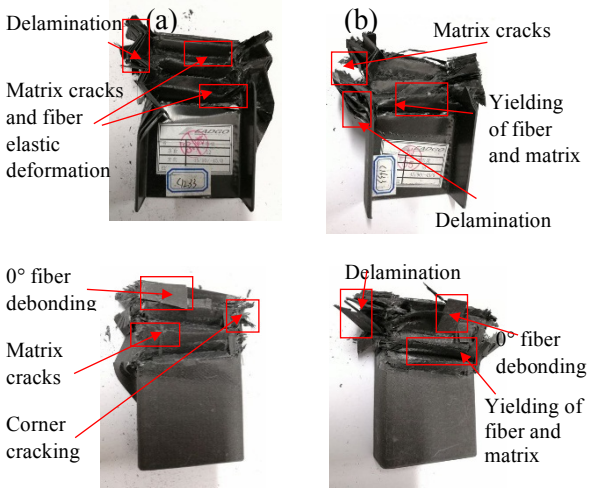

Fig 9. Failure morphology of the C-channel specimens with 45°/90°/-45°/0° ply: (a) C123; (b) C163

The load-displacement curves of thin-walled C-channels with 45°/90°/-45°/0° ply are shown in Fig.10. The amplitude of the load-displacement curve is smaller, the fluctuation is denser, and the shape of the curve is similar to a 'serrated'. In general, the load level is higher. In addition, the average crushing load does not change obviously during the crushing process.

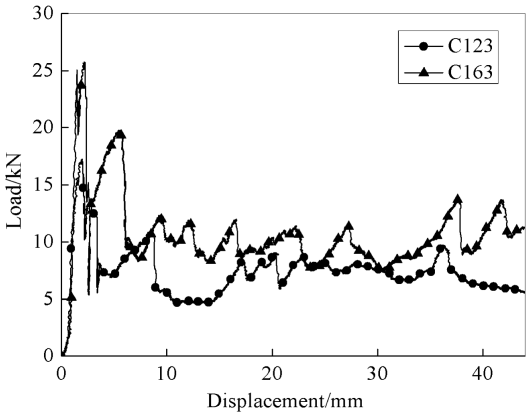

Fig 10. Load-displacement curves of C-channels with 45°/90°/-45°/0° plies

3 Axial compression stability analysis

The F_{max}, F_{mean} and *SEA* are shown in Fig.11. In general, the F_{max} is: 0°/90° > 45°/90°/-45°/0° > +45°/-45° > 0°, the F_{mean} and *SEA* of C-channels with 0°/90° and 45°/90°/-45°/0° lay-ups are larger than that with +45°/-45° lay-up. It is obvious that the F_{max}, F_{mean} and *SEA* of C-channels with unidirectional 0° plies are the smallest, which is because of the overall instable crushing manner. For C-channels with +45°/-45° lay-up, due to the absence of axial reinforcement, the predominant failure mode is matrix fracture, and resulting in a relatively small F_{max} and poor energy-absorbing performance. The F_{max} of C-channels with 0°/90° and 45°/90°/-45°/0° lay-ups are larger, which is due to the axial and circumferential reinforcement of 0° and 90° plies. When the specimen is crushed, the 0° fiber is axially compressed and failed, and the 90° fiber is pulled off by the 0° fiber, so a big axial crushing stiffness is presented. Besides, more energy is dissipated by fiber fracture, so the F_{mean} and *SEA* are also larger.

Besides, it can be seen from Fig.11(c) that the *SEA* of C161 is smaller than that of C121, which is because the C161 specimen is too thick to fold, therefore local instability occurs, resulting in local brittle fracture. Local buckling can be observed from the failure morphology in Fig.5, and the length of the buckling zone is large. Besides, serious delamination and matrix brittle fracture are also presented, resulting in a poor

ability to withstand axial crushing load. As a result, the energy absorbed by the 16-layer specimen is relatively small.

In addition, the F_{max} of C-channels with 45°/90°/-45°/0° lay-up are slightly smaller than that with 0°/90° lay-up, although they have the similar *SEA*, which indicate that the former has a better energy-absorbing characteristic. Besides, its *SEA* increases as the thickness increases, which is desired for energy-absorbing structure design and application.

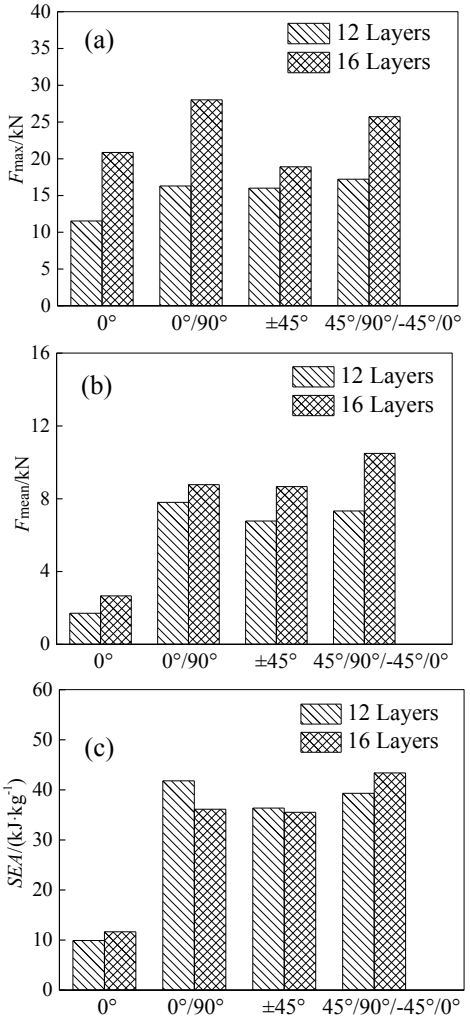

Fig.11 Energy-absorbing characteristic parameters C-channels: (a) F_{max}; (b) F_{mean}; (c) *SEA*

3 Conclusion

C-channels with unidirectional 0° plies suffer total instable failure during crushing, resulting in a low level of energy absorption; C-channels with 0°/90° and ±45°, 45°/90°/-45°/0° lay-ups undergo steady progressive crushing with matrix crack and delamination, having a relatively good energy-absorbing characteristic. Besides, for C-channels with 45°/90°/-45°/0° lay-ups, the *SEA* increases as the thickness increases, so the energy absorption behavior is controllable.

References

[1] Siromani D, Henderson G, Mikita D, et al. An experimental study on the effect of failure trigger mechanisms on the energy absorption capability of CFRP tubes under axial compression. *Composites Part A Applied Science & Manufacturing,* Vol. 1, No. 1, pp 25-35, 2014.

[2] Palanivelu S, Paepegem W V, Degrirck J, et al. Parametric study of crushing parameters and failure patterns of pultruded composite tubes using cohesive elements and seam, Part I: Central delamination and triggering modelling. *Polymer Testing*, Vol. 1, No. 1, pp 729-741, 2010.

[3] Feraboli P. Development of a modified flat-plate test specimen and fixture for composite materials crush energy absorption. *Journal of Composite Materials*, Vol. 1, No. 1, pp 1967-1990,2009.

[4] Deepak S. Crush-worthy design and analysis of aircraft structures. *Philadelphia, Pennsylvania, US: Drexel University*, 2013.

[5] Palanivelu S, Paepegem W V, Degrieck J, et al. Comparative study of the quasi-static energy absorption of small-scale composite tubes with different geometrical shapes for use in sacrificial cladding structures. *Polymer Testing*, Vol. 1, No. 1, pp 381-396, 2010.

[6] TRAN T N, HOU S, HAN X, et al. Crushing analysis and numerical optimization of angle element structures under axial impact loading. *Composite Structures*, Vol. 1, No. 1, pp 422-435, 2015.

[7] Rozylo P. Experimental-numerical test of open section composite columns stability subjected to axial compression. *Archives of Materials Science & Engineering*, Vol. 1, No. 1, pp 58-64, 2017.

[8] Meredith J, Bilson E, Powe R, et al. A performance versus cost analysis of prepreg carbon fiber epoxy energy absorption structures. *Composite Structures*, Vol. 1, No. 1, pp 206-213, 2015.

[9] Reddy A D, Rehfield L W, Bruttomesso R I, et al. Local buckling and crippling of thin-walled composite structures under axial compression. *Journal of Aircraft*, Vol. 1, No. 1, pp 97-102, 2015.

[10] Friedrich L, Loosen S, Liang K, et al. Stacking sequence influence on imperfection sensitivity of cylindrical composite shells under axial compression. *Composite Structures*, Vol. 1, No. 1, pp 750-761, 2015.

Copyright Statement